



OPEN

An inducible model for genetic manipulation and fate-tracing of PDGFR β -expressing fibrogenic cells in the liver

Florian Hamberger, Young-Seon Mederacke & Ingmar Mederacke

Myofibroblasts are the source of extracellular matrix protein during liver fibrogenesis. Fibroblasts, hepatic stellate cells (HSCs) and vascular smooth muscle cells are mesenchymal subpopulations in the liver that are characterized by the expression of PDGFR β and contribute to the pool of these myofibroblasts. Conditional knockout models are important to better understand the function of specific liver cell populations including mesenchymal cells. While there is a limited number of constitutive mouse models for liver mesenchymal cell specific transgene expression, there is no established model for inducible gene targeting in HSCs or PDGFR β -expressing mesenchymal cell populations in the liver. To address this, we investigated whether the tamoxifen inducible PDGFR β -P2A-CreER^{T2} mouse can be used as a reliable tool to specifically express transgens in liver mesenchymal cells. Our data demonstrate, that PDGFR β -P2A-CreER^{T2} specifically and efficiently marks over 90% of retinoid positive HSCs in healthy and fibrotic liver in mice upon tamoxifen injection, and that those cells give rise to *Col1a1*-expressing myofibroblasts in different models of liver fibrosis. Together with a negligible background recombination of only about 0.33%, this confirms that the PDGFR β -P2A-CreER^{T2} mouse is nearly as efficient as established constitutive *LratCre* and PDGFR β -Cre mouse models for recombination in HSCs, and that it is a powerful model for mesenchymal liver cell studies that require an inducible Cre approach.

Liver fibrosis and its end stage liver cirrhosis are a major cause of patient mortality worldwide¹. However, despite extensive research into the underlying mechanisms of fibrosis development, there are still no antifibrotic drugs to date². Hepatic stellate cells (HSCs), a pericyte-like cell population in the liver, could be identified as a dominant source of myofibroblasts in the liver independent of liver damage etiology³. Accordingly, deletion of *Col1a1* in *LratCre*-positive HSCs significantly reduced the deposition of fibrillar collagen in the liver⁴. Moreover, single-cell RNA sequencing study revealed that HSCs are not a functionally homogenous cell population, but show spatial zonation of HSCs with central-vein-associated HSCs being the dominant collagen-producing cells in contrast to portal vein-associated HSCs⁵, and that inhibition of central-vein-associated HSCs is a promising approach to therapy in non-alcoholic steatohepatitis (NASH). A recent study identified three different mesenchymal subpopulations—fibroblasts, HSCs and vascular smooth muscle cells (VSMC)—by using a platelet-derived growth factor receptor beta (*Pdgfrb*)-GFP knockin reporter mouse⁵. Research into the function and behavior of the different mesenchymal cell populations, though, is limited by the availability of animal and cell culture models. Constitutive Cre transgenic mice are available that can be used in combination with fluorescent Cre-reporter mice to study liver fibrogenic cell populations⁶. While the lecithin retinol acyltransferase (*Lrat*)-Cre transgenic mouse can be used to mark HSCs³, PDGFR β Cre transgenic mice label all mesenchymal cells populations^{6,7}. Constitutive expression can have downsides as certain gene modifications are embryonically lethal, or in the case that the timing of genetic modification is of interest⁸. In these cases, an inducible Cre would add a valuable research tool. One of the most commonly used systems for inducible Cre expression is the CreER system, which combines the Cre recombinase with a tamoxifen binding domain⁹. In this model the binding of tamoxifen, an artificial estrogen-receptor antagonist¹⁰, to the CreER fusion protein facilitates the translocation of it from the cytoplasm to the nucleus, where the Cre can exert its function. In this way the induction of Cre activity can be controlled by tamoxifen application.

Department of Gastroenterology, Hepatology, Infectious Diseases and Endocrinology, Hannover Medical School, Carl-Neuberg-Str. 1, 30625 Hannover, Germany. email: mederacke.ingmar@mh-hannover.de

As there is no established inducible mouse model for the expression of transgens in the different hepatic mesenchymal cell populations to date, we sought to investigate whether the recently published PDGFR β -P2A-CreERT2 transgenic mouse that efficiently labels pericytes in the retina and brain¹¹ also marks mesenchymal cell populations in the liver and therefore could constitute a viable model for inducible gene deletion.

Results

PDGFR β -P2A-CreERT2 efficiently labels retinoid positive HSCs in the liver upon tamoxifen induction. First, we were interested whether HSCs are efficiently labeled by PDGFR β -P2A-CreERT2. Therefore, we crossbred the PDGFR β -P2A-CreERT2 mouse line with the red fluorescent tdTomato Cre reporter mouse line to generate PDGFR β -P2A-CreERT2 x tdTomato animals. These mice were injected with tamoxifen or oil for five consecutive days. Subsequently, the liver was harvested at day 8 for either immunofluorescent staining or isolation of HSCs by cell sorting (Fig. 1A). Analysis by fluorescent microscopy did not detect any expression of tdTomato Cre reporter in oil-injected control mice. In contrast, PDGFR β -P2A-CreERT2 x tdTomato mice that received tamoxifen showed strong tdTomato expression in the majority of retinoid positive HSCs (Fig. 1B). To determine the percentage of HSCs that are labelled by PDGFR β -P2A-CreERT2, we analyzed freshly isolated HSCs by flow cytometry. In tamoxifen injected animals, we observed that a mean of $88.85 \pm 2.57\%$ HSCs (violet A positive) were also positive for tdTomato indicating a high efficiency of PDGFR β -P2A-CreERT2 for HSCs. In contrast, oil-injected PDGFR β -P2A-CreERT2 x tdTomato animals only had a very low level of tdTomato labelled HSCs ($0.33 \pm 0.47\%$), indicating a neglectable background recombination (Fig. 1C, Supplemental Fig. 1A). Furthermore, immunofluorescent staining for desmin on frozen liver sections of PDGFR β -P2A-CreERT2 x tdTomato mice showed a strong overlap of tdTomato fluorescence in untreated and fibrotic liver (Fig. 1D, Supplemental Fig. 1B–D). Importantly, PDGFR β -P2A-CreERT2 induced tdTomato expression was detected by fluorescent microscopy up to one year after tamoxifen-induction in HSCs in the liver (Supplemental Fig. 1E).

PDGFR β -P2A-CreERT2 labels HSC populations in healthy and fibrotic liver. To confirm that PDGFR β -P2A-CreERT2 mediated reporter gene expression is mainly restricted to mesenchymal cell populations in the liver, frozen liver sections of PDGFR β -P2A-CreERT2 x tdTomato mice were stained for markers of endothelial cells (CD31), macrophages (F4/80), hepatocytes (HNF4a), and cholangiocytes (cytokeratin) after tamoxifen induction. No overlap of Cre-induced tdTomato expression with macrophage, hepatocyte and cholangiocyte markers was observed (Fig. 2A,B). Furthermore, staining for the aforementioned markers was performed in PDGFR β -P2A-CreERT2 x tdTomato mice treated with six injections of CCl₄, in order to analyze whether PDGFR β -P2A-CreERT2 mediated reporter gene expression is restricted to mesenchymal cell populations in the injured liver as well. Similarly to untreated animals, no overlap of Cre-induced tdTomato fluorescence was observed with CD31, F4/80, HNF4a or cytokeratin positive cells (Fig. 2C), indicating that PDGFR β -P2A-CreERT2 does not label endothelial cells, macrophages, hepatocytes or cholangiocytes in the fibrotic liver.

PDGFR β -P2A-CreERT2-labelled mesenchymal cells give rise to myofibroblasts in toxic and cholestatic liver fibrosis. Next, we were interested whether PDGFR β -P2A-CreERT2 x tdTomato labelled mesenchymal cells in the liver transdifferentiate into myofibroblasts. Therefore, PDGFR β -P2A-CreERT2 x tdTomato were crossed with mice expressing collagen 1a1 driven GFP (ColGFP). In these triple transgenic mice, we observed a strong overlap of PDGFR β -P2A-CreERT2 driven tdTomato expression with ColGFP (marking myofibroblasts)¹² and almost complete overlap of those cells with the fibroblast marker alpha smooth muscle actin (aSMA) (Fig. 3A). This data confirms, that the PDGFR β -P2A-CreERT2 labelled cells give rise to the majority of Col1a1 positive fibrogenic cells in the liver.

To quantify the amount of PDGFR β -P2A-CreERT2-derived myofibroblasts, we used the triple transgenic PDGFR β -P2A-CreERT2 x tdTomato x Col1a1-GFP mouse and induced liver fibrosis by CCl₄. Using this approach, we observed that over 95% of Col1a1-positive myofibroblasts also expressed PDGFR β -P2A-CreERT2 induced tdTomato indicating that almost all myofibroblasts in this model were derived from PDGFR β -expressing mesenchymal cell populations (Fig. 3B). To exclude that the data may be specific to toxic liver fibrosis, two well-established models of cholestasis-induced liver fibrosis, bile duct ligation and 3,5-diethoxycarbonyl-1,4-dihydrocollidine (DDC)-containing diet, were employed. Similar to CCl₄, we observed a strong overlap of PDGFR β -P2A-CreERT2 induced tdTomato expression and Col1a1-GFP indicating that the observed effects are independent of etiology of liver damage (Fig. 3C,D). Additionally, staining for Thy1.2¹³ and Slit2¹⁴ was performed as markers of portal fibroblasts and portal fibroblasts with mesenchymal stem cell features, respectively. Thy1.2 predominantly marked cells in the portal area (Supplemental Fig. 2A–C). In the CCl₄ fibrosis model, approximately half of the Thy 1.2 positive cells were also labelled by PDGFR β -P2A-CreER (Supplemental Fig. 2B). In liver fibrosis induced by bile duct ligation, the majority of Thy 1.2 positive cells in the periportal area were also labelled by PDGFR β -P2A-CreER (Supplemental Fig. 2C). Slit2 was expressed on PDGFR β -P2A-CreERT2 positive cells, both in the liver parenchyma as well as in the portal areas (Supplemental Fig. 3A–C).

To exclude, that the continuation of Tamoxifen injections during liver injury overestimated Cre efficiency, we also analyzed overlap of PDGFR β -P2A-CreERT2 induced tdTomato expression and Col1a1-GFP in animals that received the last Tamoxifen injection prior to the induction of liver fibrosis by CCl₄. In these animals, we observed that 93.5% of Col1a1-positive myofibroblasts also expressed PDGFR β -P2A-CreERT2 induced tdTomato indicating a similar degree of PDGFR β -P2A-CreERT2 labelled cells in animals with or without continuation of Tamoxifen during liver injury (Supplemental Fig. 4).

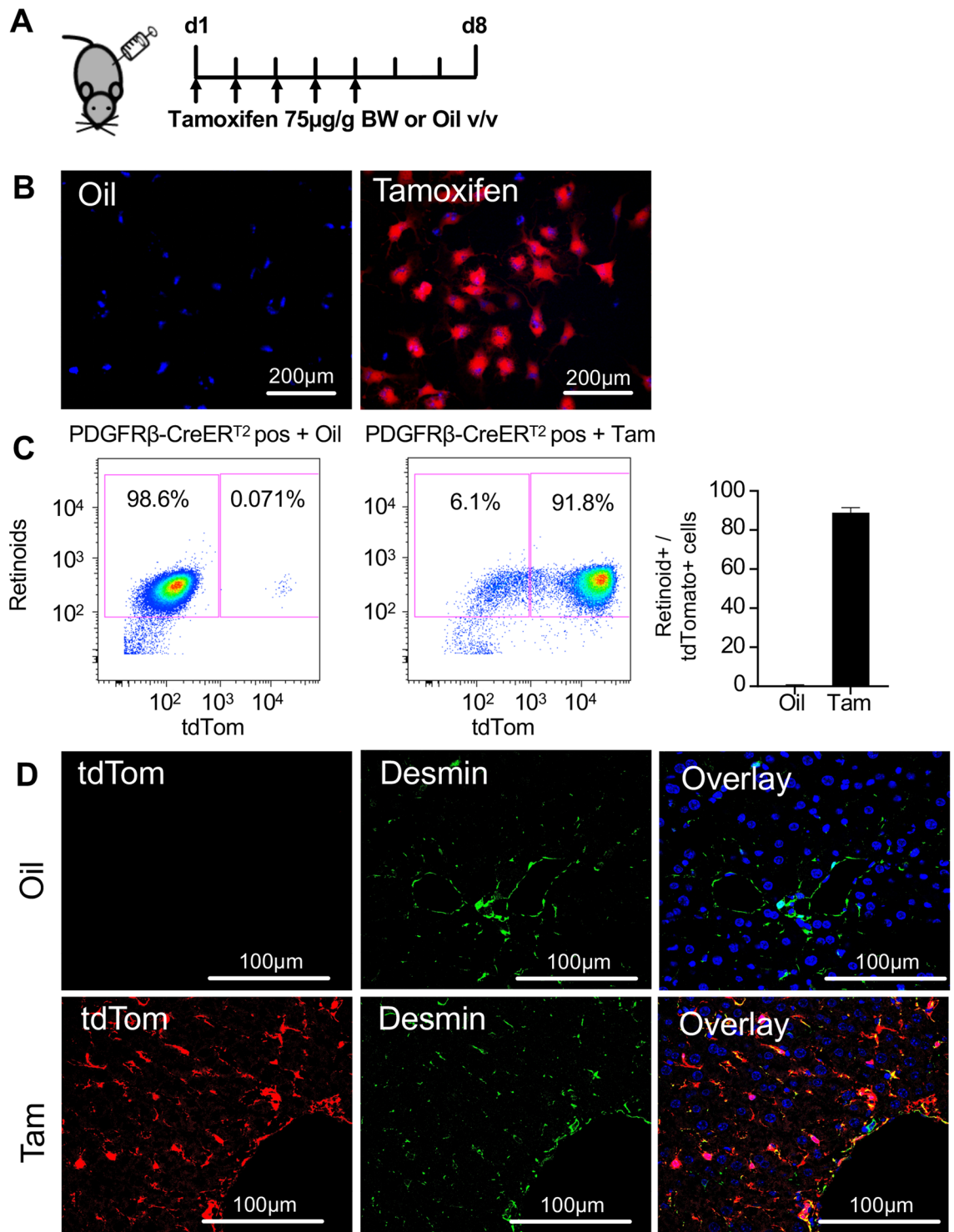


Figure 1. PDGFR β -P2A-CreER^{T2} efficiently labels retinoid positive HSCs in the liver upon tamoxifen induced Cre activation. (A) PDGFR β -P2A-CreER^{T2} mice were crossed with mice containing a tdTomato (tdTom) Cre reporter. Cre activity was induced by tamoxifen injection (i.p.) at 75 μ g/g BW for five consecutive days. Animals were sacrificed three days after the last tamoxifen or oil injection, respectively. (B,C) Fluorescent images (B) and pseudocolor plots (C) of freshly isolated HSCs from PDGFR β -P2A-CreER^{T2} x tdTomato mice that received tamoxifen or oil show Cre-mediated tdTomato expression only in tamoxifen treated animals (n=4). (D) Fluorescent staining shows co-localization of desmin with PDGFR β -P2A-CreER^{T2} induced tdTomato expression.

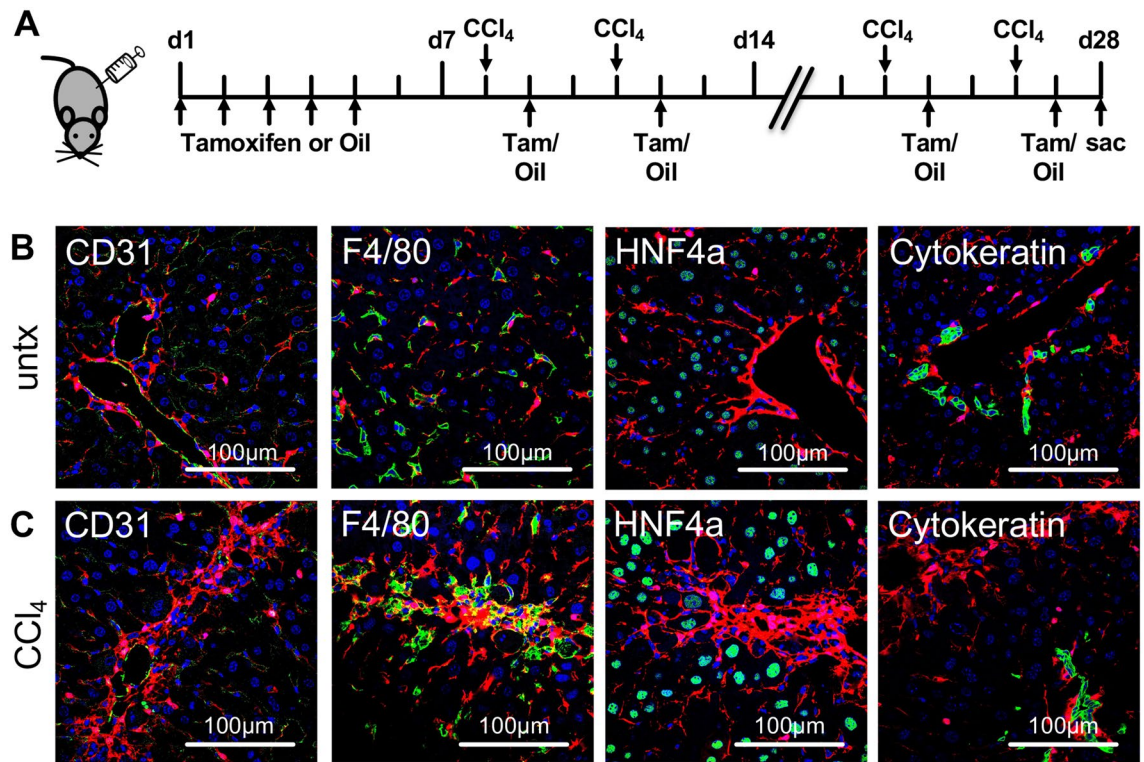


Figure 2. Tamoxifen induced tdTomato expression in PDGFR β -P2A-CreER^{T2} mice is restricted to mesenchymal cell populations. (A) PDGFR β -P2A-CreERT² was induced by tamoxifen injection (i.p.) at 75 μ g/g BW for five consecutive days. Subsequently, liver fibrosis was induced by biweekly injections of CCl₄ for a total of three weeks. Tamoxifen was continued during liver fibrosis induction. (B,C) Staining for markers of endothelial cells (CD31), macrophages (F4/80), hepatocytes (HNF4a), and cytokeratin show that PDGFR β -P2A-CreER^{T2} driven tdTomato expression is exclusive to mesenchymal cell populations both in untreated and fibrotic mice.

Discussion

The role of mesenchymal cell populations in the development of liver fibrosis has been extensively studied in the last decades^{15–19}, but oftentimes interpretation of the results is limited by the models used.

Both the Lrat- and the PDGFR β promoters were shown to label HSCs in the context of liver fibrosis of different etiologies^{3,7}. However, both the previously described LratCre and PDGFR β -Cre reporter mice have a constitutively active Cre recombinase, which limits their use. This can result in unspecific activity if the promoter is only temporarily active in the course of cell differentiation, but not specific for the differentiated cell²⁰. Furthermore, the time point of Cre activity can be a concern once a specific deletion results in cell lethality during early development.

Those concerns could be addressed by using a transgenic mouse model with inducible Cre expression. However, no such model that targets mesenchymal cell populations has been published so far. We therefore investigated whether the inducible PDGFR β -P2A-CreER^{T2} mouse¹¹ can be used as a reliable tool to express transgens in mesenchymal cell populations in the liver.

To address this question, we generated a triple transgenic mouse model containing the PDGFR β -P2A-CreER^{T2}, a red fluorescent tdTomato Cre reporter²¹, and a Col1a1-driven GFP²². Our data revealed that tamoxifen-induced activation of PDGFR β -P2A-CreER^{T2} efficiently induced reporter gene expression in pericytes of the liver, which lasted up to one year after activation. Experiments with vehicle-treated mice showed practically no reporter expression, demonstrating no significant leakiness of the PDGFR β -P2A-CreER^{T2} construct which has been observed for other CreER transgenic mice, such as the RipCreER, a beta-cell specific mouse line that can be used to manipulate gene expression in insulin-producing cells of the endocrine pancreas²³. PDGFR β -P2A-CreER^{T2} induced reporter expression was tested via immunostaining for markers of different liver resident cell types, in which fluorescent reporter expression only overlapped with desmin, a marker commonly used to stain pericytes in different organs, including HSCs^{3,24–26}. Staining for the portal fibroblast marker Thy1.2 revealed overlap with PDGFR β -P2A-CreER^{T2} induced reporter expression, which is in line with previous data showing that fibroblasts and VSMC express Thy1 to a certain extent⁵. It has been suggested that HSCs and Thy1.2 positive cells are two distinct cell populations^{13,27}, however it cannot be excluded that also some HSCs express Thy1⁵.

Furthermore, PDGFR β -P2A-CreER^{T2} induced reporter expression remained specific for mesenchymal cells even under fibrogenic conditions in the CCl₄ toxic liver fibrosis model. Overlap of alpha smooth muscle actin, a common myofibroblast marker, and overlap with endogenous collagen 1a1 driven GFP further confirmed that fibrogenic cells in the liver are PDGFR β -P2A-CreER^{T2} derived. As we achieve a high recombination of

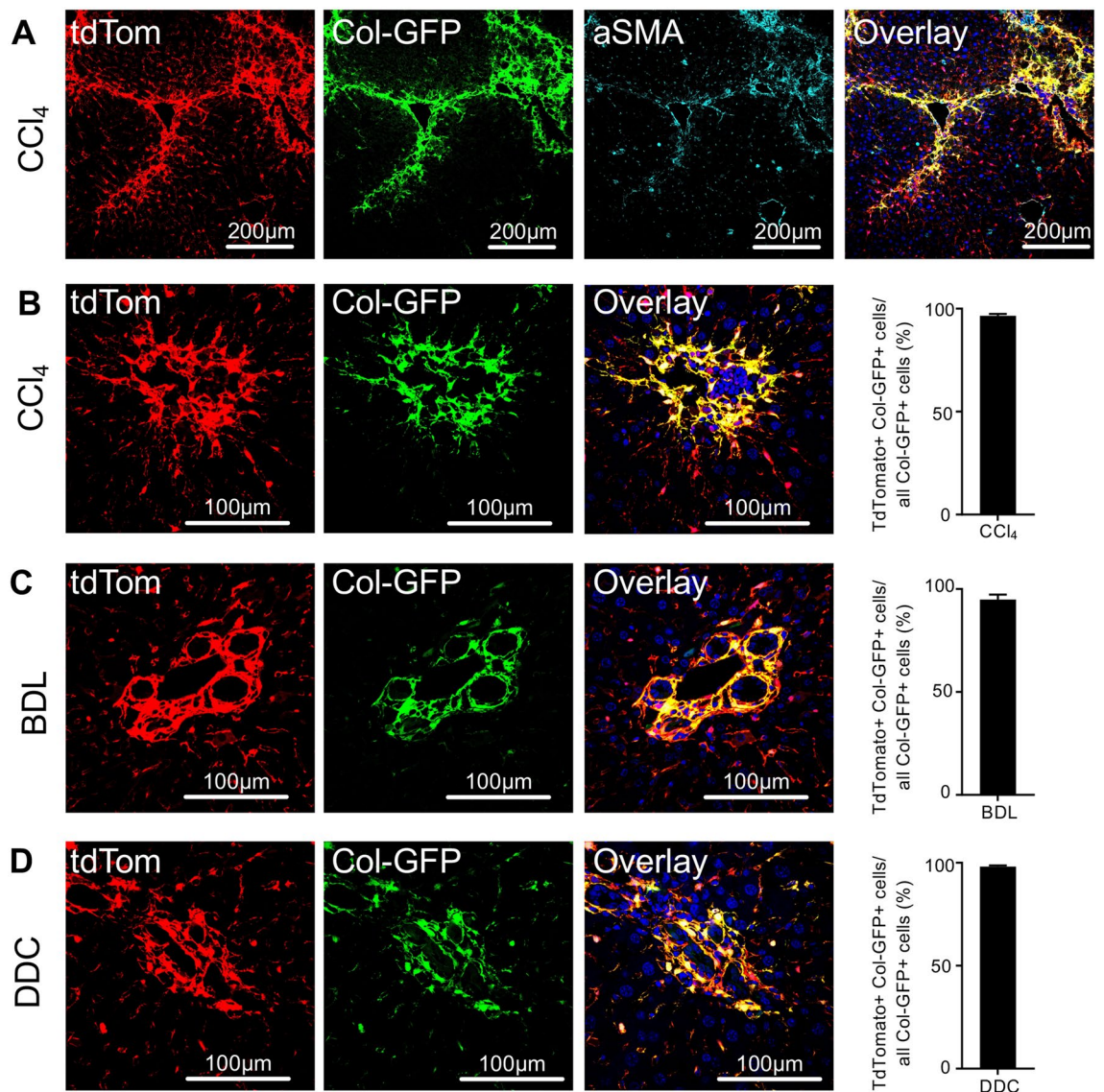


Figure 3. PDGFR β -P2A-CreER^{T2} labelled mesenchymal cell populations give rise to myofibroblasts in different models of liver injury. (A) Staining for myofibroblast marker aSMA combined with Col1a1GFP (ColGFP) overlaps with PDGFR β -P2A-CreER^{T2} driven tdTomato expression in fibrotic liver. (B–D) Co-expression of ColGFP and PDGFR β -P2A-CreER^{T2} driven tdTomato in different liver fibrosis models (CCl₄ (n = 4), bile duct ligation BDL (n = 4), 3,5-diethoxycarbonyl-1,4-dihydrocollidine DDC (n = 4)). Means \pm SEM.

PDGFR β -P2A-CreER^{T2} in retinoid positive HSCs of over 90% and a similarly high percentage of pericyte derived myofibroblasts in three different liver fibrosis models, the inducible PDGFR β -P2A-CreER^{T2} model can be used once an inducible Cre mouse model for liver mesenchymal cell populations is required with a similar efficiency as the constitutive PDGFR β Cre⁷ or the well accepted LratCre transgenic mouse model⁵.

However, PDGFR β Cre as a marker for fibrogenic cells in the liver has some limitations. In recent years, single cell RNA sequencing studies using a Pdgfrb-GFP transgenic mouse have revealed a spatial zonation of HSCs with central-vein-associated HSCs and portal vein-associated HSCs, whereby central-vein-associated HSCs were the dominant collagen-producing cells in CCl₄ induced toxic liver injury⁵. Without other markers, PDGFR β Cre cannot distinguish between these different HSC populations with distinct functions and the different PDGFR β -positive cell populations including fibroblasts, HSCs and VSMC⁵. Furthermore, another study identified several clusters of fibroblasts in the liver, with some of them (Fib-3 and Fib-4 clusters) expressing low levels of Pdgfrb and thus being underestimated in studies using Pdgfrb as a promoter for Cre recombinases or GFP¹⁴. We also performed immunohistochemistry for Slit2, a marker for portal fibroblasts with mesenchymal stem cell features (PMSCs)¹⁴. In contrast to this study, we observed Slit2 expression not only restricted to the portal area, but also in the liver parenchyma. Of note, PDGFR β -P2A-CreER^{T2} driven tdTomato expression overlapped with Slit2, both in normal and fibrotic liver indicating that Slit2 might not only be a precursor for PMSCs but also for HSCs. Further studies need to address this finding.

Nevertheless, our data demonstrates that the tamoxifen inducible PDGFR β -P2A-CreERT² mouse model is similarly efficient to the established constitutive LratCre and PDGFR β -Cre mouse models and can be applied once an inducible Cre recombinase is required to study liver fibrogenesis.

Material and methods

Mice. All animal experiments were conducted under the approval of the Lower Saxony State Office for Consumer Protection and Food Safety (LAVES, Germany; #18/3059), and in compliance with both the regulations of the German Animal Welfare Act, as well as the ARRIVE (Animal Research: Reporting of In Vivo Experiments) guidelines and regulations²⁸.

PDGFR β -P2A-CreERT² mice (Jax #030201)¹¹, and tdTomato Cre reporter mice (Jax #007909)²¹ were purchased from Jackson Laboratory. The Col1a1-GFP mouse line has been previously described¹². For breeding, we used PDGFR β -P2A-CreERT² Cre-positive males and Cre negative females. Cre activity was induced by tamoxifen injection (75 μ g/g BW intraperitoneal (i.p.)), dissolved in maizeoil (Carl Roth) for five consecutive days (Fig. 1A). Oil injected animals served as controls. In experiments where liver injury was induced, the injection of tamoxifen was continued two times a week until the end of the respective experiment.

Liver fibrosis and injury models. Toxic liver fibrosis was induced by biweekly injections of CCl₄ (0.5 μ l/g BW, dissolved in maizeoil at a ratio of 1:3) for three weeks (6 injections total). For the induction of cholestatic liver fibrosis, mice underwent ligation of the common bile duct²⁹. Briefly, after abdominal incision, the common bile duct was ligated distally. As an additional model of cholestatic liver fibrosis, mice were fed a 0.1% DDC-containing diet for 3 weeks³. At the end of the experiments, the animals were sacrificed by an overdose of a mixture of ketamine and xylazine (300 μ g ketamine + 12 μ g xylazine per g BW, i.p.) followed by cervical dislocation, after which organs were harvested for further analysis.

Isolation of hepatic stellate cells and FACS analysis. HSCs were isolated as previously described³⁰. Subsequently, freshly isolated, gradient-purified HSCs were subjected to FACS analysis. HSCs contain vitamin A with a specific fluorescence that can be detected using ultra-violet light (405–407-nm laser) for excitation and a 450/50-nm band-pass filter for detection³⁰. TdTomato was analyzed using an excitation wavelength of 560-nm and was detected at 610-nm. The gating strategy is shown in Supplemental Fig. 1A. FACS analysis was performed using a MoFlo XDP Cell Sorter (Beckman-Coulter).

Immunohistochemical staining and microscopy. Tissue from mouse liver was collected, fixed with 4% paraformaldehyde, embedded and frozen in Tissue-Tek[®] O.C.T.[™] Compound and cut to yield 7 μ m sections. Frozen liver sections were incubated with the following primary antibodies: desmin (1:200, R&D, AF3844), CD31 (1:100, Abcam, ab28364), F4/80 (1:100, Thermo, BM8), HNF4a (1:100, Cell Signaling, #3113S), cytokeratin (1:200, TROMA-III), α SMA (1:100, Abcam, ab5694), Thy1.2 (1:100, Thermo, 53-2.1) and Slit2 (1:100, Abcam, ab7665). Fluorescent secondary antibodies with different fluorescent conjugates (goat anti-rat 488 (Invitrogen, A11006), 1:200; goat anti-rabbit 488 (Invitrogen, A11034), 1:200; donkey anti-rabbit Cy5 (Novus Biologicals, NBP1-75286PECY55), 1:100; donkey anti-goat 488 (Invitrogen, A11055), 1:200) were employed followed by Hoechst 33258 staining (Sigma, B2883-100MG). All immunohistochemistry- and immunofluorescence-based quantification was performed on sections containing representative tissue from several lobes of the liver (three mid-sized tissue pieces per liver per mouse). Fluorescence images were captured employing a Nikon eclipse Ti2 microscope or DMi8 confocal laser microscope (Leica). Images were analyzed using ImageJ software (Version 1.51n).

Data availability

All data generated or analyzed during this study are included in this published article (and its Supplementary Information files).

Received: 15 November 2022; Accepted: 27 April 2023

Published online: 05 May 2023

References

- Roth, G. A. *et al.* Global, regional, and national age-sex-specific mortality for 282 causes of death in 195 countries and territories, 1980–2017: A systematic analysis for the Global Burden of Disease Study 2017. *Lancet* **392**(10159), 1736–1788 (2018).
- Fallowfield, J. A., Jimenez-Ramos, M. & Robertson, A. Emerging synthetic drugs for the treatment of liver cirrhosis. *Expert. Opin. Emerg. Drugs* **26**(2), 149–163 (2021).
- Mederacke, I. *et al.* Fate tracing reveals hepatic stellate cells as dominant contributors to liver fibrosis independent of its aetiology. *Nat. Commun.* **4**, 2823 (2013).
- Filliol, A. *et al.* Opposing roles of hepatic stellate cell subpopulations in hepatocarcinogenesis. *Nature* **610**(7931), 356–365 (2022).
- Dobie, R. *et al.* Single-cell transcriptomics uncovers zonation of function in the mesenchyme during liver fibrosis. *Cell Rep.* **29**(7), 1832–18478 (2019).
- Greenhalgh, S. N., Conroy, K. P. & Henderson, N. C. Cre-activity in the liver: Transgenic approaches to targeting hepatic nonparenchymal cells. *Hepatology* **61**(6), 2091–2099 (2015).
- Henderson, N. C. *et al.* Targeting of α 5 β 1 integrin identifies a core molecular pathway that regulates fibrosis in several organs. *Nat. Med.* **19**(12), 1617–1624 (2013).
- Yan, J. *et al.* Gli2-regulated activation of hepatic stellate cells and liver fibrosis by TGF- β signaling. *Am. J. Physiol. Gastrointest. Liver Physiol.* **320**(5), G720–G728 (2021).
- Kohan, D. E. Progress in gene targeting: Using mutant mice to study renal function and disease. *Kidney Int.* **74**(4), 427–437 (2008).
- Jordan, V. C. Tamoxifen: A most unlikely pioneering medicine. *Nat. Rev. Drug Discov.* **2**(3), 205–213 (2003).

11. Cuervo, H. *et al.* PDGFRbeta-P2A-CreER(T2) mice: A genetic tool to target pericytes in angiogenesis. *Angiogenesis* **20**(4), 655–662 (2017).
12. Yata, Y. *et al.* DNase I-hypersensitive sites enhance alpha1(I) collagen gene expression in hepatic stellate cells. *Hepatology* **37**(2), 267–276 (2003).
13. Katsumata, L. W., Miyajima, A. & Itoh, T. Portal fibroblasts marked by the surface antigen Thy1 contribute to fibrosis in mouse models of cholestatic liver injury. *Hepatol. Commun.* **1**(3), 198–214 (2017).
14. Lei, L. *et al.* Portal fibroblasts with mesenchymal stem cell features form a reservoir of proliferative myofibroblasts in liver fibrosis. *Hepatology* **76**(5), 1360–1375 (2022).
15. Henderson, N. C., Rieder, F. & Wynn, T. A. Fibrosis: From mechanisms to medicines. *Nature* **587**(7835), 555–566 (2020).
16. Sherman, M. H. Stellate cells in tissue repair, inflammation, and cancer. *Annu. Rev. Cell Dev. Biol.* **34**, 333–355 (2018).
17. Friedman, S. L. Hepatic stellate cells: Protean, multifunctional, and enigmatic cells of the liver. *Physiol. Rev.* **88**(1), 125–172 (2008).
18. Parola, M., Marra, F. & Pinzani, M. Myofibroblast - like cells and liver fibrogenesis: Emerging concepts in a rapidly moving scenario. *Mol. Aspects Med.* **29**(1–2), 58–66 (2008).
19. Higashi, T., Friedman, S. L. & Hoshida, Y. Hepatic stellate cells as key target in liver fibrosis. *Adv. Drug Deliv. Rev.* **121**, 27–42 (2017).
20. Heffner, C. S. *et al.* Supporting conditional mouse mutagenesis with a comprehensive Cre characterization resource. *Nat. Commun.* **3**, 1218 (2012).
21. Madisen, L. *et al.* A robust and high-throughput Cre reporting and characterization system for the whole mouse brain. *Nat. Neurosci.* **13**(1), 133–140 (2010).
22. Hernandez-Gea, V. *et al.* Autophagy releases lipid that promotes fibrogenesis by activated hepatic stellate cells in mice and in human tissues. *Gastroenterology* **142**(4), 938–946 (2012).
23. Liu, Y. *et al.* Tamoxifen-independent recombination in the RIP-CreER mouse. *PLoS One* **5**(10), e13533 (2010).
24. Zhang, D. *et al.* Desmin- and vimentin-mediated hepatic stellate cell-targeting radiotracer (99m)Tc-GlcNAc-PEI for liver fibrosis imaging with SPECT. *Theranostics* **8**(5), 1340–1349 (2018).
25. Hoffmann, C. *et al.* Hepatic stellate cell hypertrophy is associated with metabolic liver fibrosis. *Sci. Rep.* **10**(1), 3850 (2020).
26. Hellstrom, M. *et al.* Role of PDGF-B and PDGFR-beta in recruitment of vascular smooth muscle cells and pericytes during embryonic blood vessel formation in the mouse. *Development* **126**(14), 3047–3055 (1999).
27. Dudas, J. *et al.* Thy-1 is expressed in myofibroblasts but not found in hepatic stellate cells following liver injury. *Histochem. Cell Biol.* **131**(1), 115–127 (2009).
28. Kilkenny, C. *et al.* Animal research: Reporting in vivo experiments: The ARRIVE guidelines. *Br. J. Pharmacol.* **160**(7), 1577–1579 (2010).
29. Seki, E. *et al.* TLR4 enhances TGF-beta signaling and hepatic fibrosis. *Nat. Med.* **13**(11), 1324–1332 (2007).
30. Mederacke, I. *et al.* High-yield and high-purity isolation of hepatic stellate cells from normal and fibrotic mouse livers. *Nat. Protoc.* **10**(2), 305–315 (2015).

Acknowledgements

The Col1a1-GFP mouse line was kindly provided by Tatiana Kisseleva and David A. Brenner (University of California, San Diego, USA).

Author contributions

F.H. performed experiments, analyzed data and drafted the manuscript. Y.-S.M. contributed to data analysis and critically reviewed the manuscript. I.M. designed and supervised the study and drafted the manuscript.

Funding

Open Access funding enabled and organized by Projekt DEAL.

Competing interests

The authors declare no competing interests.

Additional information

Supplementary Information The online version contains supplementary material available at <https://doi.org/10.1038/s41598-023-34353-y>.

Correspondence and requests for materials should be addressed to I.M.

Reprints and permissions information is available at www.nature.com/reprints.

Publisher's note Springer Nature remains neutral with regard to jurisdictional claims in published maps and institutional affiliations.



Open Access This article is licensed under a Creative Commons Attribution 4.0 International License, which permits use, sharing, adaptation, distribution and reproduction in any medium or format, as long as you give appropriate credit to the original author(s) and the source, provide a link to the Creative Commons licence, and indicate if changes were made. The images or other third party material in this article are included in the article's Creative Commons licence, unless indicated otherwise in a credit line to the material. If material is not included in the article's Creative Commons licence and your intended use is not permitted by statutory regulation or exceeds the permitted use, you will need to obtain permission directly from the copyright holder. To view a copy of this licence, visit <http://creativecommons.org/licenses/by/4.0/>.

© The Author(s) 2023